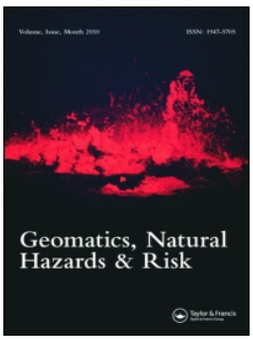

Taylor & Francis
Taylor & Francis Group

Geomatics, Natural Hazards and Risk

ISSN: 1947-5705 (Print) 1947-5713 (Online) Journal homepage: https://www.tandfonline.com/loi/tgnh20

Measurement of surface velocity in open channels using a lightweight remotely piloted aircraft system

M. Bolognesi, G. Farina, S. Alvisi, M. Franchini, A. Pellegrinelli & P. Russo

To cite this article: M. Bolognesi, G. Farina, S. Alvisi, M. Franchini, A. Pellegrinelli & P. Russo (2017) Measurement of surface velocity in open channels using a lightweight remotely piloted aircraft system, Geomatics, Natural Hazards and Risk, 8:1, 73-86, DOI: 10.1080/19475705.2016.1184717

To link to this article: https://doi.org/10.1080/19475705.2016.1184717

Published online: 17 May 2016.

GEOMATICS, NATURAL HAZARDS AND RISK, 2017
VOL. 8, NO. 1, 73–86
http://dx.doi.org/10.1080/19475705.2016.1184717

Taylor & Francis
Taylor & Francis Group

REVIEW ARTICLE

OPEN ACCESS

Measurement of surface velocity in open channels using a lightweight remotely piloted aircraft system

M. Bolognesi, G. Farina, S. Alvisi, M. Franchini, A. Pellegrinelli and P. Russo

Engineering Department In Ferrara (ENDIF), University of Ferrara, Ferrara, Italy

ABSTRACT

In this paper, a low-cost remotely piloted aircraft system (RPAS) technique is proposed for measurement of the surface velocity in rivers or channels with low surface velocity and small discharge. To verify the reliability of the results obtained with the RPAS, we simultaneously measured the surface velocity with other methods based on total stations and close range photogrammetry. The RPAS was used both with ground control points (GCPs) for orientation of the photographic images and without GCPs. The data analysis showed that the RPAS provides valid results even without GCPs. Use of a RPAS without GCPs, relying solely on flight altitude to determine the water velocity, opens the way for its utilization in emergency conditions when it is impossible to access the river banks for the realization and survey of GCPs.

ARTICLE HISTORY
Received 19 November 2015
Accepted 27 April 2016

KEYWORDS
Water surface velocity; UAV; measurement; RPAS

1. Introduction

River discharge estimation plays a fundamental role in a number of fields: it is essential for planning a rational and responsible use of water resources, ensuring that they are correctly and adequately managed, controlling flood events and mitigating hydraulic risks. In common practice, discharge estimation methods are indirect, since they rely on flow point velocity measurements within the cross-section, whose bathymetry is assumed to be known.

The velocity-area method is one of the most widely used discharge measurement techniques (UNI EN ISO 748 2008): it requires knowledge of the cross-sectional geometry and current meter measurements at different depths along a sufficient number of verticals located within the flow area. While the velocity-area method is particularly reliable, it turns out to be laborious, time-consuming and costly because of the considerable commitment of equipment and personnel, with poor accuracy close to the riverbed due to the presence of vegetation. Moreover, strong currents, which typically occur during exceptional flood events, may cause danger to operators or prevent completion of the velocity sampling.

A valid alternative for discharge estimation is the entropy method: it is based on the principle of entropy maximization and has been used in different fields of research to derive the probability density function of a specific random variable. This approach was applied for the first time to open channel hydraulics by Chiu (1987, 1988) to identify the corresponding (probability) distribution of flow velocity, from which a linear relationship between the mean velocity and the maximum velocity u_{max} in a river cross-section is derived as a function of a dimensionless parameter M (Chiu 1991;

CONTACT M. Bolognesi blgmcl@unife.it

Xia 1997), i.e.

$$\overline{U} = f(M, u_{\max}) \tag{1}$$

From a practical viewpoint, the dimensionless parameter M must be preliminarily estimated in order to convert the maximum velocity $u_{\max}$ into the mean section velocity $\overline{U}$.

In this regard, Farina et al. (2014) proposed a procedure requiring only the maximum surface velocity measurement to estimate the parameter M. Therefore, the possibility of indirectly deriving discharge from the maximum velocity recorded on the surface would not only drastically reduce the measurement times and costs but would eliminate the problems related to monitoring with traditional techniques and instruments (such as current meters), particularly during major floods.

However, the maximum surface velocity must be estimated with sufficient accuracy. The simplest and most practical technique for surface velocity measurement relies on the use of 'non-contact' radar sensors based on the Doppler effect (Costa et al. 2000; Melcher et al. 2002; Cheng et al. 2004; Costa et al. 2006; Fulton & Ostrowski 2008). Although radar sensors are accurate instruments, their application is restricted to velocities exceeding 0.2−0.3 m/s. Thus, we are unable to measure velocity via radar sensors in drainage systems characterized by slow currents.

Alternative 'non-contact' approaches for surface velocity measurement are based on particle image velocimetry (PIV) (Adrian 1991; Adrian 2005). This methodology has been adopted in several hydrological studies to deduce the displacement field of natural tracers (foam, leaves) or artificial tracers added to the surface to carry out measurements with a fixed camera installed on a roof (Creutin et al. 2003), on a bridge (Muste et al. 2008; Tauro et al. 2016), on a telescopic rod (Jodeau et al. 2008) or on a tripod (Tauro, Grimaldi et al. 2012; Tauro, Mocio et al. 2012), which allows for surface flow monitoring at a limited number of locations. Recently, significant efforts have been made to extend PIV to manned (Fujita & Hino 2003; Fujita & Kunita 2011) and remotely piloted aircraft systems (Pagano et al. 2014; Tauro, Pagano et al. 2015; Tauro, Petroselli et al. 2015): the main advantage is the ability to rapidly characterize water flow systems in large areas that can be difficult to access by human operators. Because of the low cost of remotely piloted aircraft system (RPAS) and the significant progress in navigation systems and on-board sensors, remote sensing from an RPAS, previously used in cultural heritage surveying (Bolognesi et al. 2014), is now widely used in environmental sciences. There are numerous data acquisition applications: monitoring of aquatic vegetation (Derkx et al. 2015), surveillance of a watercourse (Baroux & Gardes 2015), evaluation of areas suitable for infrastructure construction (Viguier & Forest 2015) and estimation of river discharge (Detert & Weitbrecht 2015).

With regard to river discharge, a remarkable advantage of an RPAS is that it allows non-contact measurements of surface velocity in wide rivers during a flood event with inaccessible areas, which make fixed measurement implementations impractical. Nevertheless, applications of an RPAS to estimate surface water velocity are very limited in number and are typically related to natural rivers with maximum surface speeds of 2−2.5 m/s (Detert & Weitbrecht 2015; Fujita & Kunita 2011).

In this paper, a low-cost RPAS technique is proposed for measurement of the maximum surface velocity in rivers or channels with low surface velocity and small discharge. The measurement technique is based on photogrammetry, in particular the processing of sequences of digital images taken at low altitude, which reflect the different positions of one or more floats in time during their movement along the channel. The data processing is very simple and does not require specialized software.

This method allows reconstruction of the distribution of the surface velocity when several floats are positioned in the channel across the flow width; with only one float, it allows determination of the maximum surface velocity only after prior verification of where the maximum velocity occurs. However, since it is well known that the maximum surface velocity occurs approximately at the centreline of the flow width in a prismatic section (Chiu & Lin 1983; Chiu 1988; Chow et al. 1988;

Chiu & Tung 2002), a single float located at the centre of the examined watercourse allows maximum surface velocity estimation.

The technique was applied in two test channels with small cross-sections and low surface velocity. To verify the reliability of the results obtained with the RPAS, we simultaneously measured the surface velocity with three other methods based on total stations, close range photogrammetry and radar gun. Nevertheless, only the first two were used in comparisons because the sensitivity of the radar gun proved inadequate for measurement of such low surface velocity.

The proposed survey technique could easily be used in situations of environmental emergency, when time is limited and access to flooded zones is both difficult and risky. This technique is also advantageous in very wide rivers and in the absence of bridges, when measurement of the maximum speed at the centre is extremely difficult.

2. Test sites

The proposed method was verified using data from two channels of the drainage system managed by the Consorzio di Bonifica Pianura di Ferrara: Fossa Masi (Masi Torello) in Figure 1 and Valle Isola (Comacchio) in Figure 2. They were selected because they are easily accessible, have low flow velocity typical of drainage channels, and feature downstream hydraulic devices (gate or pumping station) which allow easy and reliable discharge estimation.

Fossa Masi is a 'mixed-use' channel because its behaviour varies according to the different seasonal uses. While in winter (October–March) the channel is almost empty and used to drain off excess rainwater from surrounding farmland, its capacity inevitably decreases in summer

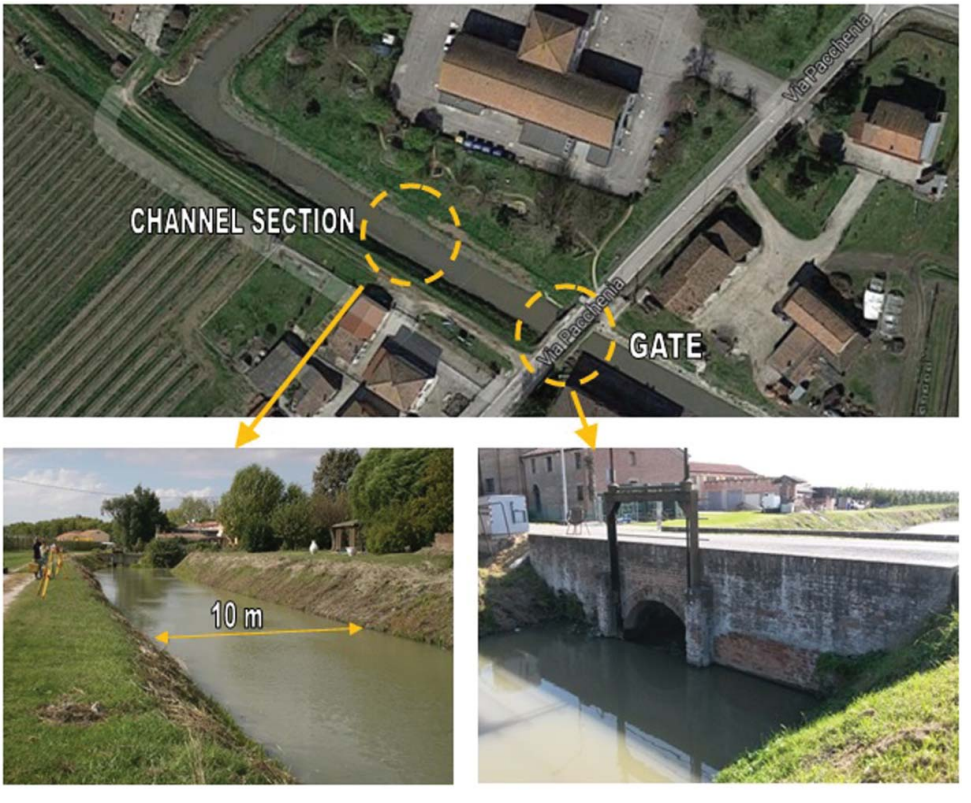

Figure 1. Fossa Masi channel (Masi Torello). In particular, it is observed the segment of the channel considered for this study and the gate located downstream near the bridge.

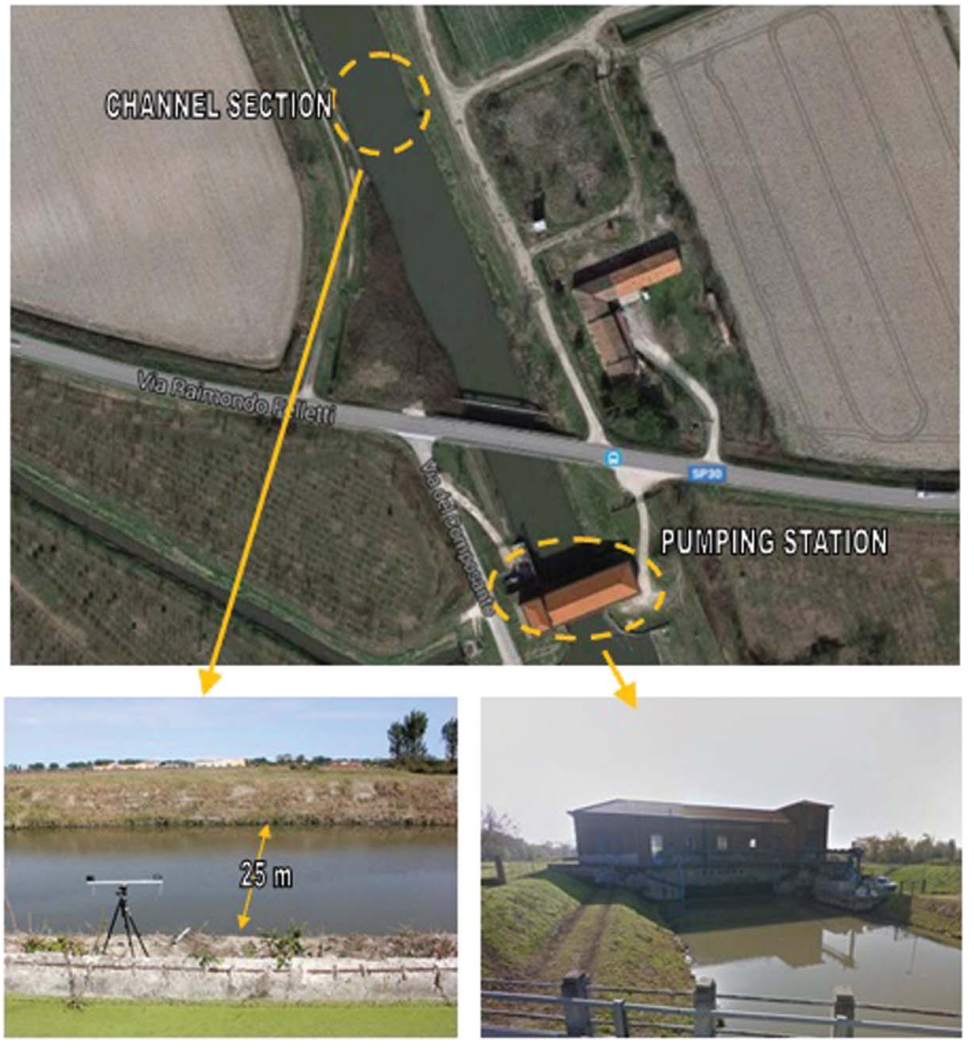

Figure 2. Valle Isola (Comacchio). It is observed the section considered for this study (lower left image) and the Guagnino pumping station, located south of the drainage basin, at about 60 m downstream.

(April−September) because irrigation water is fed into it and several gates located along the channel can be used to maintain the desired water level necessary for irrigation. Being partially water-filled, Fossa Masi has less capacity than in winter, so that if it rains the gates are opened to control the flow, the channel empties and its drainage efficiency increases.

The segment considered for this study is upstream of a gate located near a bridge (Figure 1). During winter this gate is maintained totally elevated, without intercepting the flow, while in summer it is lowered to maintain the desired volume of water in the channel. During the velocity measurement, the gate was lowered totally and its lower end lay on the cement sill on the channel bottom near the bridge, thus behaving as a gate weir.

Valle Isola collects the water of the whole channel system serving the Valle Isola drainage area adjacent to the Ferrara seaside. This channel flows through the drainage area from north to south and carries the water to the Guagnino pumping station (Figure 2). This station, located south of the drainage basin, mechanically raises the water to sea level with different groups of pumps and a maximum discharge of 17.9 m^3/s. The segment considered for this study is located very close to the pumping station, about 60 m upstream.

In both channels we identified two cross-sections as parallel to each other as possible and perpendicular to the main direction of the channel in order to delimit a segment where velocity measurements were carried out. The two segments considered for this study are straight and of uniform cross-section and slope, with a stable bed and margins; they are sited far enough from the weir and the Guagnino pumping station, respectively, to avoid unsteady flow conditions during measurements.

In prismatic sections of channels with the characteristics listed above, it has been amply demonstrated that the distribution of surface velocity is approximately symmetric, with the maximum value located more or less at the centreline of the flow width. Therefore, we preliminarily verified the symmetry of the velocity distribution by analyzing the movement of several floats across the whole width of the channels; it was confirmed that the maximum velocity occurred in the centre zone of the flow width. In view of these results, we considered the transit of single floats located at the centreline of the flow width to estimate the maximum surface velocity. Only one velocity measurement was performed for the first site, while two campaigns were carried out for Valle Isola, corresponding to the following configurations of the Guagnino pumping station:

- configuration C1 with one active pump and discharge of 3.5 m^3/s;
- configuration C2 with two active pumps and discharge of 5.1 m^3/s.

Obviously, the higher the discharge the greater the flow velocity.

A few days before the tests, the bathymetry was measured at one of the end sections and the value was considered representative of the whole investigated segment. The cross-sections of both channels are shown in Figure 3.

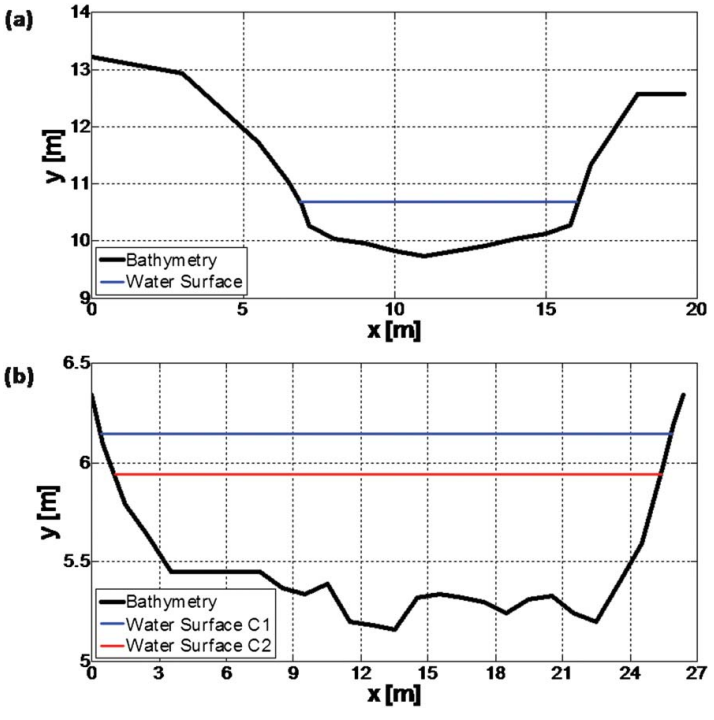

Figure 3. Cross-sections of the test channels: (a) Fossa Masi and (b) Valle Isola. During the velocity sampling the channels were partially water-filled: the water depth was only 1 m while the water width was 10 and 25 m for Fossa Masi and Valle Isola, respectively. The configurations C1 and C2 in Valle Isola are referred to two different configurations of the Guagnino pumping station.

The reliability of the measurements of maximum superficial velocity depended on the assumption that the motion of the floating object was as uniform as possible, located in the centre of the channel and directed parallel to the channel's central axis. To ensure that this assumption was achieved we conducted multiple repetitions of the tests and rejected those not meeting the requirements.

3. Determination of surface velocity via total stations and close range photogrammetry

To validate the RPAS technique, we applied three alternative measurement methods at both test sites to be carried out at the same time as the RPAS survey; for this we used a 'non-contact' radar sensor (radar gun), two total stations and a couple of cameras. Moreover, we used some small artificial floats made of polystyrene and plastic, with an approximately parallelepiped shape, that met the following requirements: be easily identified on images taken from the RPAS and from the ground and maintain the same speed as the water without being affected by wind.

The method based on total stations is simple and accurate. In correspondence of each of the two cross-sections of the channel, we set-up a total station with the line of sight lying on the vertical plane of the section (Figure 4). Before the start of the survey, several floats were thrown into the channel near the centre so that they could be carried by the stream. To determine the exact moment when the floating object crosses the reference section it is sufficient to observe its passage through the reticule of the total station's telescope. The time interval Δt between the passage of any float from the first to the second total station reference plane was measured with a stopwatch (with an a priori standard error of 0.1 s). Since the distance Δs between the sections is known (with an a priori standard error of 5 mm) the average speed $\overline{v}_{ts}$ of the moving float is computed as follows:

$$\overline{v}_{ts} = \frac{\Delta s}{\Delta t} \tag{2}$$

Table 1 shows the results of several determinations of the velocity in both channels and the corresponding standard deviation obtained from error propagation for uncorrelated variables. In view of the accuracy of the method, the results obtained with total stations were assumed as reference values for other tests.

At the same time as the total stations measurements, a photogrammetric survey was performed with a device consisting of a bar set parallel to the channel with two cameras (CANON Powershot SX130) with parallel optical axes perpendicular to the axis of the channel (Figure 5).

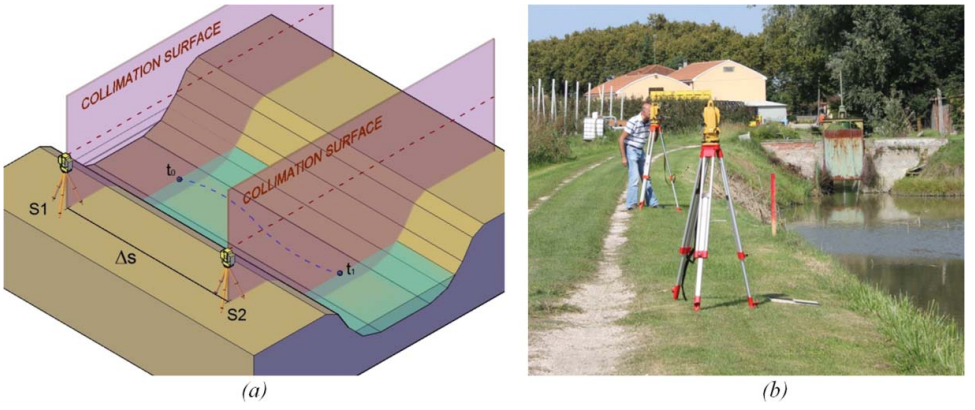

Figure 4. Layout of the total stations survey: (a) vertical reference planes (line of sight) and (b) set-up of the instruments on the bank of the channel.

Table 1. Surface velocity values obtained via total stations and estimated standard deviations. 250 × 58 mm (96 × 96 DPI).

Channel	Δs	Δt	$\overline{v}_{ts}$	σ_v
	(m)	(s)	(m/s)	(mm/s)
Fossa Masi	16.51	485.5	0.034	0.01
Valle Isola (C1)	13.53	78.2	0.173	0.23
Valle Isola (C2)	13.53	50.1	0.270	0.55

With two identical cameras with the same focal distance, the field of view (L) is the same (L1 = L2) and the base B (in this case 0.906 m) is constant regardless of the distance between the cameras and the floats (7.9 m in Fossa Masi and 15.8 m in Guagnino). The test procedure is described in Figure 6. In particular, the time Δt that the float takes to travel along the base is

$$\Delta t = t_1 - t_0 \tag{3}$$

where t_0 is the instant in which the object exits the field of view of the left camera (L1) and t_1 is the instant in which the object exits the field of view of the right camera (L2).

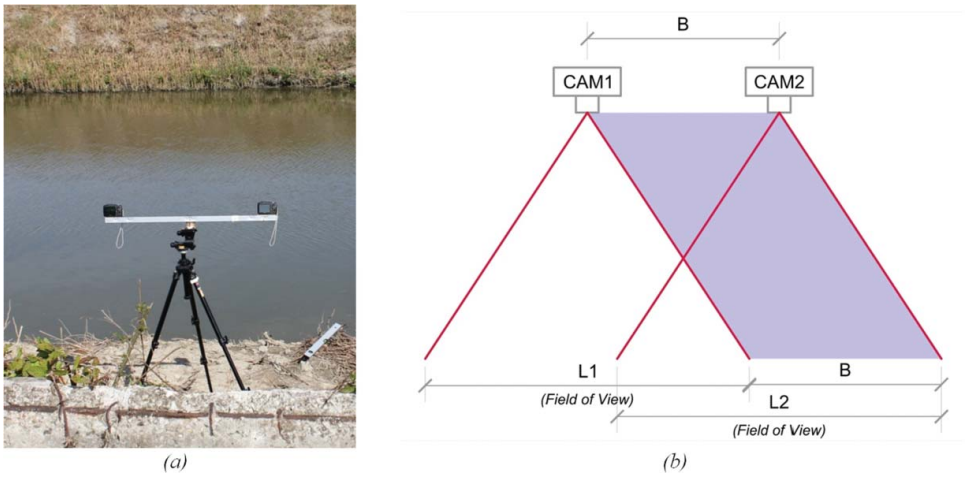

Figure 5. Photogrammetric device and geometric scheme of measurement.

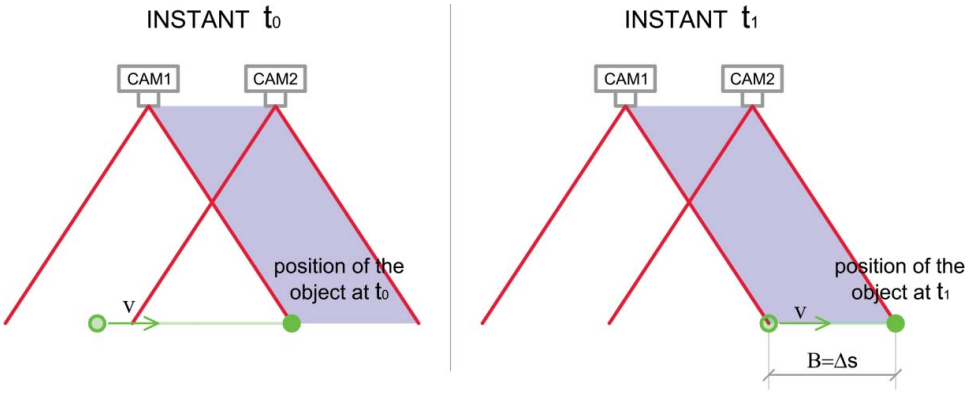

Figure 6. Scheme of the velocity measurement via the photogrammetric technique.

Table 2. Surface velocity values resulting from photogrammetry. 251 × 57 mm (96 × 96 DPI).

Channel	$B = \Delta s$	Δt	$\overline{v}_{\text{cam}}$	σ_v
	(m)	(s)	(m/s)	(mm/s)
Fossa Masi	0.906	24.5	0.037	0.25
Valle Isola (C1)	0.906	4.8	0.187	4.07
Valle Isola (C2)	0.906	3.2	0.280	8.98

Table 3. Comparison of average speeds obtained via total stations and photogrammetry. The last column reports the percentage difference of the estimated velocities. 265 × 62 mm (96 × 96 DPI).

Channel	$\overline{v}_{\text{cam}}$	$\overline{v}_{ts}$	$\lvert\Delta v\rvert_{\text{cam-}ts}$	Difference
	(m/s)	(m/s)	(m/s)	(%)
Fossa Masi	0.037	0.034	0.003	8.8
Valle Isola (C1)	0.187	0.173	0.014	8.1
Valle Isola (C2)	0.280	0.270	0.010	3.7

Hence the average surface velocity is

$$\overline{v}_{\text{cam}} = \frac{\Delta s}{\Delta t} = \frac{B}{\Delta t} \tag{4}$$

To obtain the necessary images we acquired two videos with a resolution of 1280 × 720 pixels and a focal length of 5 mm. By analyzing the extracted frame (29 frames/s) we could determine very precisely the two instants when the floaters were out of sight in the two images.

The values obtained with the photogrammetric method and the corresponding standard deviations (with a priori standard error of 0.1 s and 5 mm for the time and distance values, respectively) are listed in Table 2.

This method is valid if some simple assumptions are met: the axes of the cameras must be parallel and, as mentioned at the end of Section 2, the direction of the floating objects must be straight and parallel to the camera bar. To prevent erroneous results, we performed numerous tests and measurements for which the assumptions were not met were rejected.

Many radar gun measurements were made in both channels but reliable results were not obtained due to the low water velocity, below the sensitivity of the Doppler technique.

The results obtained with total stations and photogrammetry were compared. As seen in Table 3, the differences are very small, both in absolute and percentage terms, confirming the reliability of both techniques.

4. Determination of surface velocity via RPAS

Simultaneously with the measurements by total stations and photogrammetry, we carried out measurements with the remotely piloted aircraft system. For this experiment, we used a DJI S800 RPAS equipped with a calibrated CANON EOS M mirrorless camera with a focal length of 18.688 mm. The camera was mounted on the RPAS with a gimbal that keeps the optical axes nadiral to the ground (Figure 7). The RPAS was maintained at a constant height of 30 m over the first channel (Fossa Masi) and 50 m over the second (Valle Isola), with GSD (ground sample distance) of 8 mm in the first case and 13 mm in the second. The images had a resolution of 5184 × 3456 pixels. The difference in height between the two tests was due to the need to get both sides of the channel into every digital image in order to orient them on the basis of GCPs (ground control points). All images were corrected for optical distortion by a careful process of self-calibration carried out with the photogrammetric software Photomodeler®. For this measurement technique we employed the same floats used with the total stations and photogrammetry.

(a) (b)

Figure 7. (a) The RPAS DJI S800 used for the test and (b) a moment of the flight over the Fossa Masi channel.

4.1. Determination of surface velocity with GCPs

Four targets were positioned on the banks of the channel, two on the left and two on the right, at a distance such that all were visible in each photographic image (Figure 8). These targets would then be used as GCPs during orientation of the images. Moreover, their three-dimensional positions were detected in a local reference system with a total station with an estimated standard error about 5 mm lower than the GSD. In the same reference system we measured the height of the water surface with a total station. For each flight, sequences of about 100 images were acquired by setting the camera in the 'time lapse' mode between shots. Time lapses of 2 and 3 s were set for the tests. For each image we used Photomodeler® to determine: the orientation parameters in the local reference system (realized by GCPs), the size of the GSD and the position of any float. Hence the displacement Δs of the float in the direction of the axis of the channel between two successive instants is obtained from the vector whose components are the coordinate differences between two images acquired at time

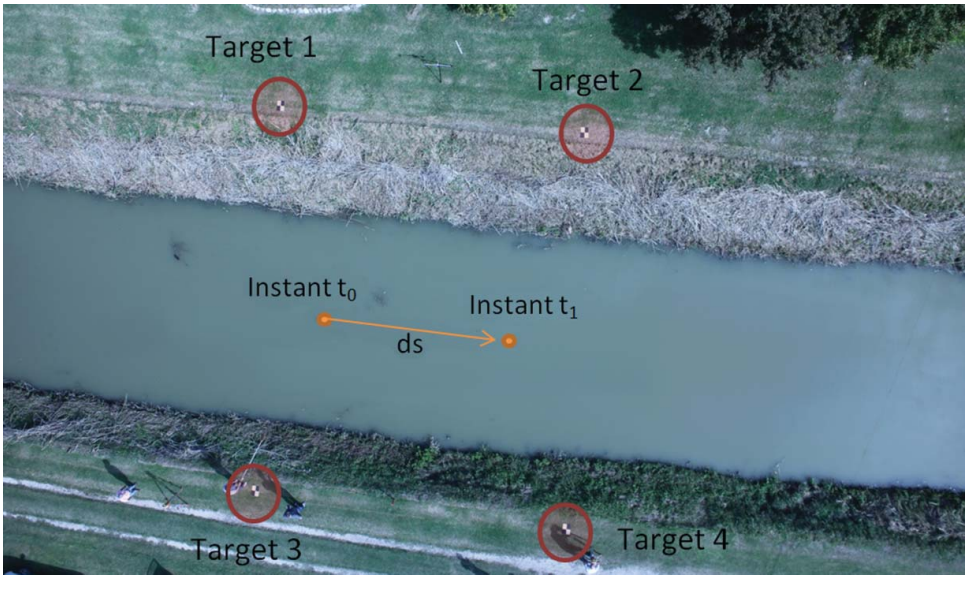

Figure 8. Layout of the test site for surface velocity measurement using the RPAS (Fossa Masi channel).

Table 4. Average surface velocity from RPAS measurements. 266 × 61 mm (96 × 96 DPI).

Channel	Δs	Δt	$\overline{v}_{uav}$
	(m)	(s)	(m/s)
Fossa Masi	1.72	40	0.043
Valle Isola (C1)	8.84	54	0.164
Valle Isola (C2)	11.19	45	0.248

interval Δt. The value of the average speed is obtained for any pair of images and any float by the ratio between Δs and Δt.

Table 4 reports the average values of surface velocity resulting from numerous measurements carried out with all the floats available for the test.

4.2. Determination of surface velocity without GCPs

The results obtained in Section 4.1 show that it is possible to detect the water surface velocity as long as GCPs are used for the orientation of frames taken with the RPAS. However, in the case of an environmental emergency or wide rivers/channels, it may be difficult or even impossible to use GCPs. Therefore, at least the flight altitude from which to calculate the scale of the frame must be known. If the RPAS remains still during the test, the flight altitude does not vary over time and the reference system is determined merely by the optical centre of the camera. The measurement of the space travelled by the float does not require an absolute reference system. The RPAS stability is an important aspect to be verified. A first check of the flight stability of the RPAS was carried out by analyzing the change of its coordinates obtained from the external orientation of images (image geo-referencing by GCPs as described in Section 4.1). A data set of 16 images taken from the Valle Isola (C1) test at regular intervals of 3 s for a total of 48 s was analyzed. The coordinate values are reported in Figure 9.

The average flight altitude is 50.42 m with a standard deviation of 0.36 m and a range of about 1.10 m. The horizontal position has a standard deviation of 0.162 m eastward and 0.144 m northward, with a range of no more than about 50 cm. A variation of flight altitude of about 1.10 m corresponds to a variation of GSD of about 0.25 mm. To determine the surface velocity we performed a simulation assuming a constant flight altitude of 50 m above the ground and 53.12 m above the

Image	East	North	Altitude
	(m)	(m)	(m)
1	4.855	23.810	51.035
2	4.749	23.637	50.959
3	4.962	23.546	50.949
4	4.783	23.515	50.817
5	4.855	23.600	50.171
6	4.744	23.818	49.936
7	4.574	23.896	50.011
8	4.633	23.704	50.107
9	4.595	23.744	50.170
10	4.538	23.660	50.145
11	4.679	23.492	50.156
12	4.701	23.462	50.364
13	4.872	23.396	50.631
14	4.994	23.624	50.377
15	5.103	23.814	50.430
16	4.905	23.637	50.449

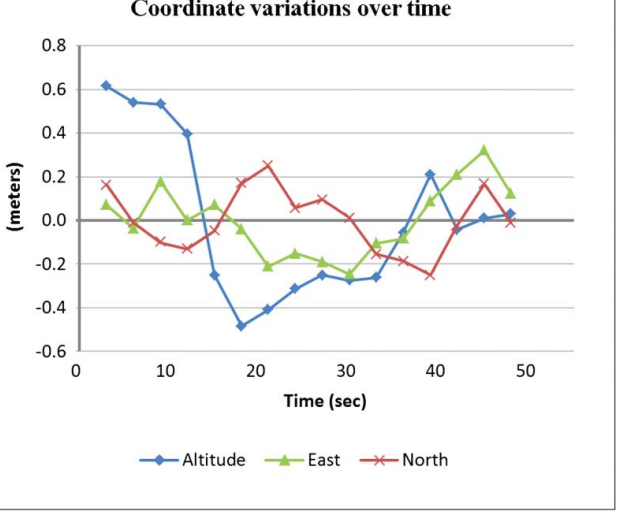

Figure 9. Coordinates of the centre of the camera and variations over time (Valle Isola (C1) test)

Interval	Δs (m)	Δt (s)	$\bar{v}_{uav}$ (m/s)
1	0.559	3	0.186
2	0.277	3	0.092
3	0.666	3	0.222
4	0.302	3	0.100
5	0.424	3	0.141
6	0.524	3	0.174
7	0.427	3	0.142
8	1.050	3	0.350
9	0.542	3	0.180
10	0.427	3	0.142
11	0.669	3	0.223
12	0.353	3	0.117
13	0.561	3	0.187
14	0.340	3	0.113
15	0.691	3	0.230

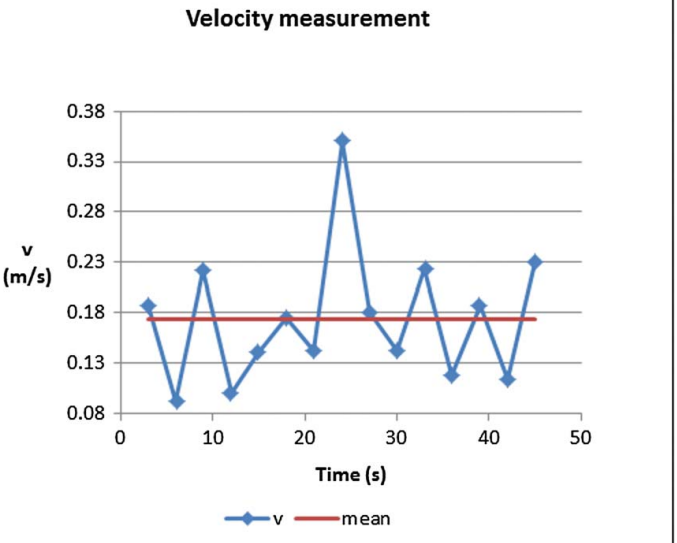

Figure 10. Method M1, velocity obtained by measurements between images taken every 3 s.

water surface. From the focal length (18.668 mm) and pixel size of the camera's sensor (0.0044 mm), we obtained a GSD of 0.0125 m. The position of the float in the image is given by the position of the corresponding pixel in a reference system fixed to the CCD (charged-coupled Device)/ CMOS (complementary metal-oxide-semiconductor) sensor. Thus in each image it is possible to measure the pixel position of the float (using the correct image without distortion) and to easily calculate the distance travelled by the object between two successive times. With these assumptions and not knowing the orientation of the images, it is not possible to evaluate the position of the float in an absolute reference system. Hence its position at each instant was determined from its pixel coordinates on each image. The distance travelled (Δs) was obtained from the difference between these coordinates. It is clear that a possible displacement of the RPAS between one image and the other would lead to a change of scale (for vertical displacement) of the image and an error of the horizontal position of the float (for horizontal displacement). The objective of the simulation was to identify the best procedure for image processing to minimize the effect of the position error of the RPAS on the calculation of the water surface velocity. For the Valle Isola (C1) test, two different calculation methods were used: in the first method (M1) we measured the velocity between images taken every 3 s; in the second method (M2) we calculated the velocity for increasing intervals between the first image and all subsequent ones.

With method M1 (see Figure 10) we obtained an average velocity of 0.174 m/s. A result like this involves long data processing because it is necessary to acquire a large number of images and to correct the distortion and make a measurement for each one. As seen in Figure 9, the distances travelled by the float in just 3 s are very small (0.28−1.05 m) and thus fluctuations in the position of the RPAS (comparable with those distances) significantly influence the estimate of the velocity. However, such fluctuations appear to be random and tend to compensate each other, as demonstrated by the fact that the average velocity is in line with the one obtained by the other techniques. This suggests that larger measuring intervals would tend to minimize the influence of the RPAS fluctuations with respect to the motion of the float. To confirm this, we performed measurements with progressively larger intervals (method M2) and observed the respective velocity results.

With method M2 (see Figure 11) the average velocity was 0.153 m/s. As the measurement interval increases, the estimated velocity approaches the calculated average value. This means that both

Interval	Δs (m)	Δt (s)	$\bar{v}_{uav}$ (m/s)
1	0.559	3	0.186
2	0.823	6	0.137
3	1.485	9	0.165
4	1.763	12	0.146
5	2.148	15	0.143
6	2.666	18	0.148
7	3.040	21	0.144
8	3.910	24	0.162
9	4.031	27	0.149
10	4.456	30	0.148
11	5.097	33	0.154
12	5.420	36	0.150
13	5.856	39	0.150
14	6.188	42	0.147
15	6.865	45	0.152

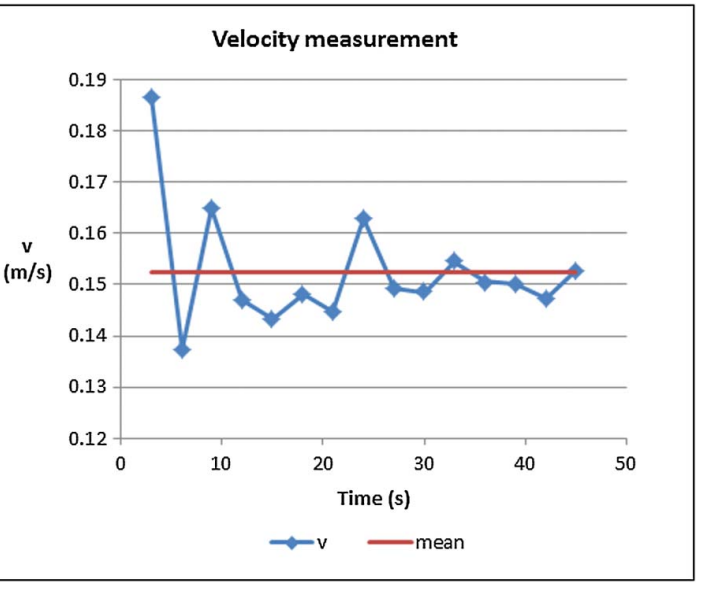

Figure 11. Method M2, velocity is calculated for increasing intervals between the first image and all subsequent ones.

methods can be used for the velocity estimation, although the second (M2) is more practical because reliable results can be obtained with only two images, one at the start and one at the end of the test.

4.3. Comparison

The comparison of the measurements made with the RPAS, with total stations and with photogrammetry is shown in Table 5.

The surface velocity estimation carried out with the RPAS with GCPs is in good agreement with those obtained with total stations for the Valle Isola 1 and 2 tests ($\Delta v < 10\%$), while there is a remarkable difference in percentage with respect to the Fossa Masi test ($\Delta v = 26.5\%$). However, this result is probably due to the very low water velocity. In fact the difference between the absolute values of the estimated velocity is only 0.009 m/s.

Table 6 compares the results obtained only with the RPAS. The velocity estimation can be performed with both calculation schemes, i.e. even without the use of GCPs, as long as there is a sufficient number of velocity determinations. In conclusion, both proposed methods seem reliable and the fluctuations of the RPAS position are considered acceptable for the purpose of the measurement.

Table 5. Comparison of average velocities obtained via total stations, photogrammetry and RPAS. (with GCPs) 266 × 64mm (96 × 96 DPI).

	Total stations	Photogrammetry vs. total stations		RPAS with GCPs vs. total stations	
Channel	(m/s)	(m/s)	(%)	(m/s)	(%)
Fossa Masi	$v = 0.034$	$v = 0.037$	$\Delta v = 8.8$	$v = 0.043$	$\Delta v = 26.5$
Valle Isola (C1)	$v = 0.173$	$v = 0.187$	$\Delta v = 8.1$	$v = 0.164$	$\Delta v = 5.2$
Valle Isola (C2)	$v = 0.270$	$v = 0.280$	$\Delta v = 3.7$	$v = 0.248$	$\Delta v = 8.1$

Table 6. Comparison of average velocities obtained by RPAS with and without GCPs. 265 × 37 mm (96 × 96 DPI).

	With GCPs	No GCPs − method M1		No GCPs−method M2	
Channel	(m/s)	(m/s)	(%)	(m/s)	(%)
Valle Isola (C1)	$v = 0.164$	$v = 0.174$	$\Delta v = 6.1$	$v = 0.153$	$\Delta v = 6.7$

5. Conclusions

The use of an RPAS to determine the maximum water surface velocity, for the purpose of estimating its flow, was tested in two channels with small cross-sections and low water velocity. To validate the results obtained with the RPAS we also determined the surface velocity via total stations and a photogrammetric survey from the ground carried out with a special device. In particular, the RPAS method was carried out both with GCPs for orientation of the photographic images and without GCPs.

The use of a RPAS provides satisfactory results even without GCPs (with minor differences of 10%) as long as there are appropriate numbers of separate velocity determinations.

In this experiment we made use of special floats, although natural objects such as driftwood could be used provided they are not affected by wind. The action of wind is particularly important when the water velocity is very low.

The use of an RPAS without GCPs, relying solely on telemetry to determine the water velocity, opens the way for its utilization in emergency conditions when it is impossible to access the river banks for the realization and survey of GCPs.

As regards the hydraulic aspect, measurement of the maximum surface velocity allowed estimation of the discharge by means of the method proposed by Farina et al. (2014). This method allows estimation of the discharge based only on the maximum water surface velocity since the channel cross-section is known. It is noteworthy that, in both case studies, a ca. 10% uncertainty in the measurement of the maximum water surface velocity leads to a similar 10% uncertainty in the estimation of the discharge. However, this uncertainty value is acceptable for practical purposes and is not significantly higher than the uncertainty that typically characterizes discharge measurements, even when much more time-consuming approaches (e.g. the velocity-area method) are used (UNI EN ISO 748 2008; Alvisi et al. 2014). Therefore, a clear advantage can be derived from using the Farina et al. (2014) method to monitor channel discharge given that RPAS data are now available and suitable for the measurement of water surface velocities. This procedure reduces the times and costs of taking measurements and ensures the maximum safety of personnel.

Acknowledgments

The authors wish to thank Consorzio di Bonifica di Ferrara for providing river basin data and CNR IRPI for technical support during the surveying.

Disclosure statement

No potential conflict of interest was reported by the authors.

References

Adrian RJ. 1991. Particle-imaging techniques for experimental fluid-mechanics. Annu Rev Fluid Mech. 23:261–304.
Adrian RJ. 2005. Twenty years of particle image velocimetry. Exp Fluids. 39:159–169.
Alvisi S, Barbetta S, Franchini M, Melone F, Moramarco T. 2014. Comparing grey formulations of the velocity-area method and entropy method for discharge estimation with uncertainty. J Hydroinform. 16:797–811.
Baroux M, Gardes J. 2015. Long endurance mini-drone for river monitoring providing crisis and territories management service. Drones and Hydraulics, at the Service of Water Professionals; Paris (France).
Bolognesi M, Furini A, Russo V, Pellegrinelli A, Russo P. 2014. Accuracy of cultural heritage 3D models by RPAS and terrestrial photogrammetry. Int Arch Photogramm. Remote Sens Spatial Inf Sci. XL-5:113–119.
Cheng RT, Gartner JW, Mason RR, Costa JE, Plant WJ, Spicer KR, Haeni FP, Melcher NB, Keller WC, Hayes K. 2004. Evaluating a radar-based, non-contact streamflow measurement system in the San Joaquin River at Vernalis, California. Menlo Park (California): U.S. Geological Survey.
Chiu LC. 1987. Entropy and probability concepts in hydraulics. J Hydraul Eng. 113:583–600.
Chiu LC. 1988. Entropy and 2-D velocity in open channels. J Hydraul Eng. 114:738–756.
Chiu LC. 1991. Application of entropy concept in open channel flow study. J Hydraul Eng. 117:615–628.

Chiu CL, Tung N. 2002. Maximum velocity and regularities in open-channel flow. J Hydraul Eng. (Special issue: stochastic hydraulics and sediment transport). 128:390–398.
Chiu CL, Lin GF. 1983. Computation of 3-D flow and shear in open channels. J Hydraul Eng. 109:1424–1440.
Chow VT, Maidment DR, Mays LW. 1988. Applied hydrology. Singapore: McGraw-Hill.
Costa JE, Spicer KR, Cheng RT, Haeni FP, Melcher NB, Thurman EM. 2000. Measuring stream discharge by non-contact methods: a proof-of-concept experiment. Geophys Res Lett. 27:553–556.
Costa JE, Cheng RT, Haeni FP, Melcher N, Spicer KR, Hayes E, Plant W, Hayes K, Teague C, Barrick D. 2006. Use of radars to monitor stream discharge by noncontact methods. Water Resour Res. 42:W07422.
Creutin JD, Muste M, Bradley AA, Kim SC, Kruger A. 2003. River gauging using PIV techniques: a proof of concept experiment on the Iowa River. J Hydrol. 277:182–194.
Derkx F, Vinçon-Leite B, Lemaire BJ, Soudani K, Quiblier C, Freissinet C, Chollet S, Derenciere B, Seguy L, Buttigieg S, et al. 2015. A drone for monitoring phytoplankton blooms in lentic aquatic environments. Drones and Hydraulics, at the Service of Water Professionals; Paris (France).
Detert M, Weitbrecht V. 2015. A low-cost airborne velocimetry system: proof of concept. J Hydraulic Res. 53:532–539.
Farina G, Alvisi S, Franchini M, Moramarco T. 2014. Three methods for estimating the entropy parameter M based on a decreasing number of velocity measurements in a river cross-section. Entropy. 16:2512–2529.
Fujita I, Hino T. 2003. Unseeded and seeded PIV measurements of river flows videotaped from a helicopter. J Visualization. 6:245–252.
Fujita I, Kunita Y. 2011. Application of aerial LSPIV to the 2002 flood of the Yodo River using a helicopter mounted high density video camera. J Hydro Environ Res. 5:323–331.
Fulton J., Ostrowski J. 2008. Measuring real-time streamflow using emerging technologies: radar, hydroacoustics, and the probability concept. J Hydrol. 357:1–10.
Jodeau M, Hauet A, Paquier A, Le Coz J, Dramais G. 2008. Application and evaluation of LS-PIV technique for the monitoring of river surface velocities in high flow conditions. Flow Meas Instrum. 19:117–127.
Melcher NB, Costa JE, Haeni FP, Cheng RT, Thurman EM, Buursink M, Spicer KR, Hayes E. 2002. River discharge measurements by using helicopter-mounted radar. Geophys Res Lett. 29:41-1–41-4.
Muste M, Fujita I, Hauet A. 2008. Large-scale particle image velocimetry for measurements in riverine environments. Water Resour Res. 44:W00D19.
Pagano C, Tauro F, Porfiri M, Grimaldi S. 2014. In: ASME, American Society of Mechanical Engineers. Development and testing of an unmanned aerial vehicle for large scale particle image velocimetry. Proceedings of the ASME Dynamic Systems and Control Conference; San Antonio (TX). (DSCC2014-5838).
Tauro F, Grimaldi S, Petroselli A, Porfiri M. 2012. Fluorescent particle tracers for surface flow measurements: a proof of concept in a natural stream. Water Resour Res. 48:W06528.
Tauro F, Mocio G, Rapiti E, Grimaldi S, Porfiri M. 2012. Assessment of fluorescent particles for surface flow analysis. Sensors. 12:15827–15840.
Tauro F, Olivieri G, Petroselli A, Porfiri M, Grimaldi S. 2016. Flow monitoring with a camera: a case study on a flood event in the Tiber River. Environ Monit Assess. 188:118.
Tauro F, Pagano C, Phamduy P, Grimaldi S, Porfiri M. 2015. Large-scale particle image velocimetry from an unmanned aerial vehicle. IEEE/ASME Trans Mechatron. 20:3269–3275.
Tauro F, Petroselli A, Arcangeletti E. 2015. Assessment of drone-based surface flow observations. Hydrol Processes. 30: 1114–1130.
UNI EN ISO 748. 2008. Hydrometry-measurement of liquid flow in open channels using current meters or floats. Reference number ISO. 748.
Viguier F, Forest O. 2015. Hydraulic risk management by coupling Lidar data and drone photography in order to construct a new high speed line. Drones and Hydraulics, at the Service of Water Professionals; Paris (France).
Xia R. 1997. Relation between mean and maximum velocities in a natural river. J Hydraul Eng. 123:720–723.